




Research Article

# Preparation and properties of porous diatomite-supported multi-walled carbon nanotubes with $\text{Na}_2\text{SO}_4 \cdot 10\text{H}_2\text{O}$ -based phase change energy storage composites

Xin Liu<sup>1</sup> · Jian Tie<sup>2</sup> · Jiqing Zhang<sup>1</sup> · Siyuan Jiang<sup>1</sup> · Shengnian Tie<sup>1</sup> 

© Springer Nature Switzerland AG 2019

## Abstract

The  $\text{Na}_2\text{SO}_4 \cdot 10\text{H}_2\text{O}$ -based phase change energy storage materials (PCMs) were fabricated through vacuum impregnating and adsorbing the oxidized multi-walled carbon nanotubes (MWCNs) with diatomite. The Fourier Transform Infrared Spectroscopy results reveals that the existence of carboxyl and hydroxyl groups in MWCNs can increase its compatibility with PCMs. The vacuum impregnated to obtain the diatomite composite PCMs (PCMs-M-D) crystallize adhering to the treated diatomite (DI-2) observed from the scanning electron microscope. The PCMs-M-D displays negligible supercooling and the thermal conductivity reaches  $0.97 \text{ W m}^{-1} \text{ K}^{-1}$ . Moreover, after 100 cycles of phase change, the melting latent heat loss is 1.43% and the solidification latent heat loss is 11.15%, showing good heat storage performance and chemical stability.

**Keywords** Porous diatomite ·  $\text{Na}_2\text{SO}_4 \cdot 10\text{H}_2\text{O}$  · PCMs · Multiwalled carbon nanotubes · Heat conductivity · Undercooling

## 1 Introduction

Phase change energy storage technology is to improve the ambient temperature by absorbing and releasing a large amount of heat in the phase change process of phase change materials [1–3]. Qinghai province, located on the Qinghai-Tibet plateau, has a large amount of mirabilite ( $\text{Na}_2\text{SO}_4 \cdot 10\text{H}_2\text{O}$ ) resources in salt lakes. As a low temperature PCMs,  $\text{Na}_2\text{SO}_4 \cdot 10\text{H}_2\text{O}$  has the advantages of small phase volume change, high latent heat density and large thermal conductivity [4]. However, it belongs to solid–liquid PCMs. For solid–liquid PCMs, the packaging technology is particularly important. PCMs is encapsulated in porous materials by natural impregnation. In general, organic PCMs compounded with porous materials include fatty acids, alkanes, polymers and their binary or ternary eutectic mixtures. Inorganic PCMs mainly include sulfate, nitrate, carbonate and metal, etc. [5, 6]. The main preparation methods of this kind of composite PCMs are vacuum impregnating, melt intercalation, melting adsorption and

so on. As the supporting material of composite PCMs, porous materials can be the existing porous agents, such as mineral materials, expanded graphite, etc., or foam metals, porous ceramics, nano carbon materials, etc. [7, 8]. Diatomite has porous structure and high porosity, with chemical stability, wear resistance, heat resistance, water absorption, permeability and other properties, can adsorb PCMs, make the PCMs does not leak in the phase change process, at the same time give some mechanical properties of PCMs. Diatomite is a natural mineral material with abundant reserves, low cost and simple mining technology. At present, there are still some problems in the research of diatomite matrix composite PCMs, such as low energy storage density and low thermal conductivity [9].

Xi et al. [10] prepared energy storage composites by using diatomite/paraffin PCMs and wood flour/high density polyethylene as secondary packaging materials. The results show that diatomite has abundant voids, and these isolated voids are less than  $10 \mu\text{m}$ . The diatomite/paraffin PCMs shows excellent stability and the use of wood

✉ Shengnian Tie, tieshengnian@163.com | <sup>1</sup>Chemical Engineering College and New Energy (Photovoltaic) Industry Research Center, Qinghai University, Xining, China. <sup>2</sup>College of Physics and Electronic Information Engineering, Qinghai Normal University, Xining, China.



SN Applied Sciences (2019) 1:710 | <https://doi.org/10.1007/s42452-019-0675-1>

Received: 22 April 2019 / Accepted: 27 May 2019 / Published online: 11 June 2019

powder/high density polyethylene as secondary packaging material completely solves the problem of liquid leakage. Xinxing [11] fabricated calcium chloride hexahydrate/diatomite/paraffin composite PCMs via impregnating calcium chloride hexahydrate into diatomite and coating it with paraffin. The test shows that diatomite has a larger nucleation surface, the supercooling degree of hydrate salt is weakened, and the stratification phenomenon of 100 cycles phase is reduced. Due to the interaction of hydration bond, capillary force, surface tension and paraffin coating, the thermal stability and reliability of the coated composite PCMs are better than that of the hydrated salt. After 100 cycles, the melting and crystallization enthalpies of coating composite PCM decreased from 108.2 and 98.5 J g<sup>-1</sup> to 106.2 and 93.8 J g<sup>-1</sup>, respectively, by 1.8% and 4.8%. Coating composite phase change material has good thermal performance, thermal reliability and chemical stability, and is a promising phase change material for thermal energy storage applications.

Herein, the Na<sub>2</sub>SO<sub>4</sub>·10H<sub>2</sub>O hydrate prepared by our research group as PCMs [12, 13], using diatomite as carrier, adding nucleating agent and water-based multi-walled carbon nanotubes, a new type of composite shaped Na<sub>2</sub>SO<sub>4</sub>·10H<sub>2</sub>O-PCMs with low supercooling, high thermal conductivity and excellent thermal storage performance was prepared through using the unique porous structure and excellent natural adsorption of diatomite,

## 2 Experimental

### 2.1 Preparation of multi walled carbon nanotubes (MWCNs)

Firstly, MWCNs (5 g) (> 95%, inner diameter: 3–5 nm, outer diameter: 8–15 nm, length: ~ 50 μm, aladdin) were added into the mixed solution of K<sub>2</sub>S<sub>2</sub>O<sub>8</sub> (8 g), P<sub>2</sub>O<sub>5</sub> (8 g), and H<sub>2</sub>SO<sub>4</sub> (25 mL, 98%) in a round long-necked beaker, and the obtained mixture was reacted at 80 °C for 5 h in

water bath. Subsequently, after being diluted to 500 ml with deionized water and placed for 12 h to separate the precipitate and the liquid, the solution was filtered and the precipitate was dried at 45 °C for 2 days. Thirdly, the precipitate (2 g) was dispersed into the H<sub>2</sub>SO<sub>4</sub> (150 mL) in water bath at 0, following by the addition of the KMnO<sub>4</sub> (25 g). After reacting for 4 h, 250 mL of deionized water was added to reduce the reactor temperature to below 50 °C, another 1 L of deionized water and 30 ml of H<sub>2</sub>O<sub>2</sub> (30 wt%) were added to prevent the reaction. Finally, the obtained mixture was taken out and placed for 2 h, washed with deionized water and air drying for 3–5 days. The treated MWCNs was labelled as MWCNs-O.

### 2.2 Preparation of porous diatomite

After being calcined at 400 °C for 4 h, the diatomite (20 g) was soaked in 20 wt% H<sub>2</sub>SO<sub>4</sub> solution at 80 °C for 2 h, following by treated with 5 wt% NaOH solution at 70 °C for 8 min and washed with distilled water. The original and the treated diatomite were defined as DI-1 and DI-2, respectively.

### 2.3 Preparation of PCMs-M-D

In this experiment, Na<sub>2</sub>SO<sub>4</sub>·10H<sub>2</sub>O-based composite phase change energy storage materials were prepared by the research group as previously described [10] the Na<sub>2</sub>SO<sub>4</sub>·10H<sub>2</sub>O (46.2 g), Na<sub>2</sub>CO<sub>3</sub>·10H<sub>2</sub>O (1.78 g), NaCl (2 g), borax (2 g), CMC (0.75 g), and sodium hexametaphosphate (0.05 g) were weighted and vacuum impregnated to obtain the diatomite composite phase energy storage material with high thermal conductivity, labelled as PCMs-M-D. 13.305 g PCMs-M can be adsorbed with 4 g DI-2 added, the adsorption rate was 67%. The detailed preparation process was schematic displayed in Fig. 1.

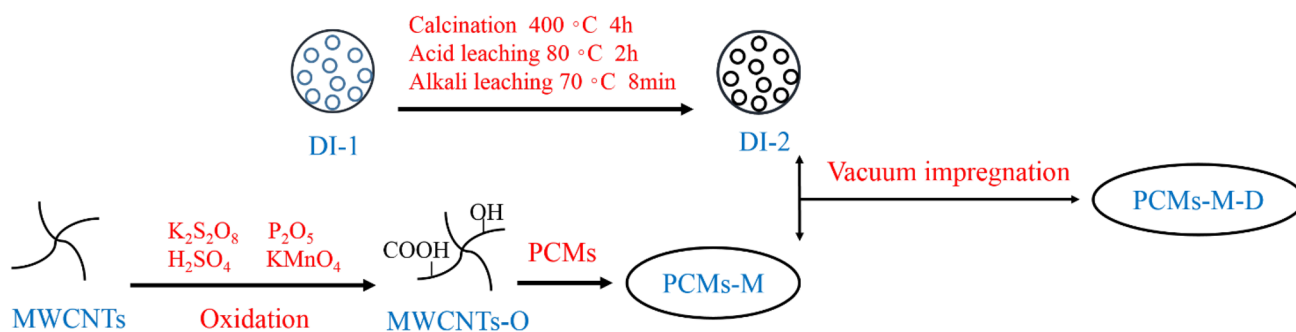


Fig. 1 Schematic illustration of the preparation process of the PCMs-M-D

### 3 Analysis methods

The morphology of the samples was characterized by low vacuum scanning electron microscope (SEM, JSM-5610 LV). The thermal constants of the composite phase change energy storage materials were analyzed with a thermal constant analyzer (TCA, TPS 2200) produced by HOT DISK in Sweden. The latent heat of the composite phase change energy storage materials was analyzed using a differential scanning calorimeter (DSC) produced by NETZSCH (Germany). The temperature was raised from 0 to 40 °C and then decreased to −5 °C at a rate of 1 °C/min in nitrogen atmosphere (50 mL/min). The phase change energy storage material was tested in a high- and low-temperature test chamber (Beijing Suri) with the temperature increasing from 0 to 40 °C and then decreased to −5 °C for 100 times. The Infrared Spectrometer manufactured was used for infrared detection of MWCNTs (FTIR, Nexus, American). The phase analysis of the material was carried out by x-ray diffractometer (XRD, D/MAX2500, Japanese).

## 4 Results and discussions

### 4.1 Fourier Transform Infrared Spectroscopy (FTIR)

Figure 2 shows the FTIR spectra of MWCNTs and MWCNTs-O. As shown in Fig. 2, after being oxidized with  $K_2S_2O_8$ ,  $P_2O_5$ ,  $H_2SO_4$ ,  $KMnO_4$ , the MWCNTs-O demonstrates two distinct peaks at 3434.28 and 1633.65  $cm^{-1}$ , which can be ascribed to the stretching vibration of hydroxyl and C=O of carboxyl group. The carboxyl group and hydroxyl group can form

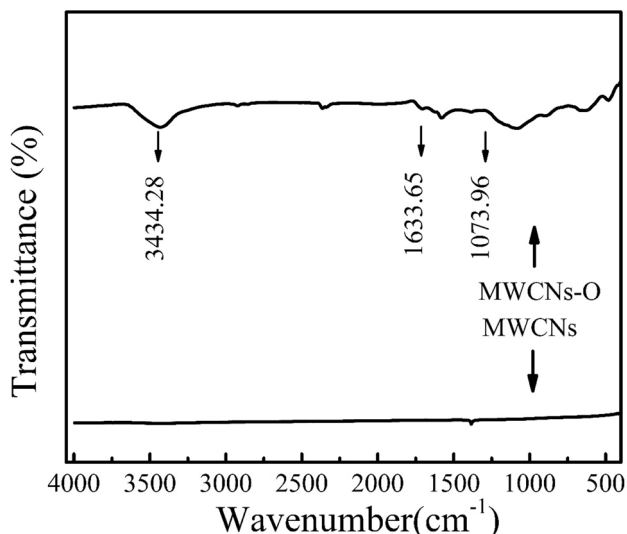


Fig. 2 Infrared Spectra of MWCNTs and MWCNTs-O

hydrogen bonds by themselves or with each other, and the higher the degree of oxidation, the more hydrogen bonds, leading to the blue shift of C=O occurs to some extent. After the oxidation treatment, hydroxyl and carboxyl groups were formed on the surface of MWCNTs-O, making it more hydrophilic, which could be well integrated with PCMs to improve the heat absorption and release efficiency.

### 4.2 Pore size analysis of diatomite

The pore characteristics of the diatomite were examined with  $N_2$  adsorption/desorption measurements. Figure 3a shows the resulting isotherm. It can be seen that both the DI-1 and DI-2 display typical II isotherms with the adsorption curve rising slowly in the front section, and rising sharply in the back section. There is no adsorption

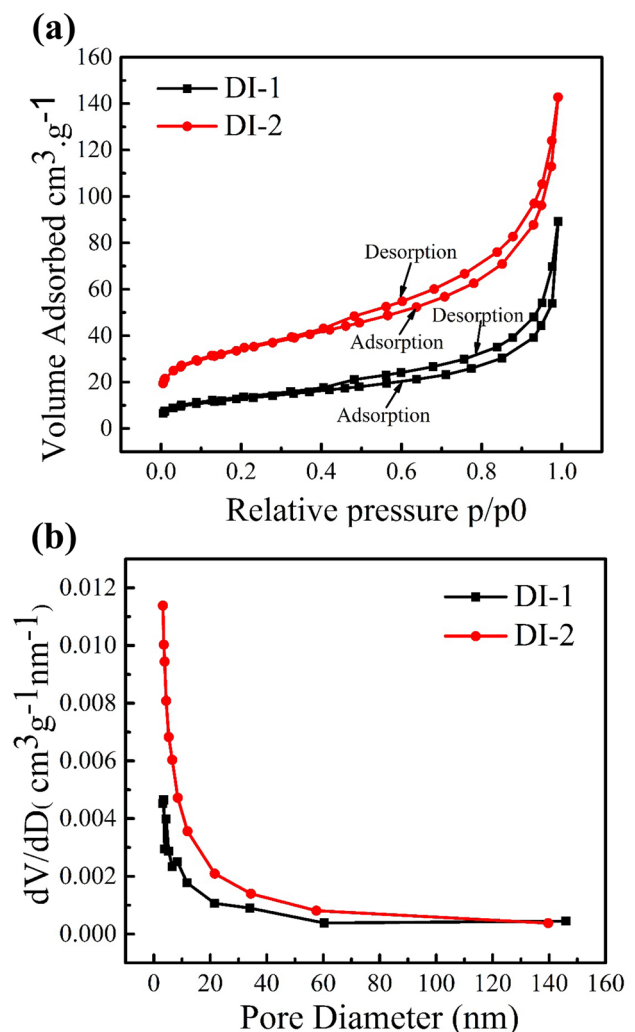


Fig. 3 a  $N_2$  adsorption/desorption isotherms and b the corresponding pore size distribution of diatomite

saturation until the relative pressure is close to 1.0, indicating that the capillary aggregation of diatomite occurs during the process of nitrogen adsorption. The type II isotherm shows that it is a macroporous solid adsorbed by multi-molecular layers. In the transition stage from monolayer to multi-molecular layer at 0–0.4 (p/p<sub>0</sub>), in the stage multilayer adsorption at 0.4–0.9 (p/p<sub>0</sub>), it shows a sharp rise at 0.9–1.0 (p/p<sub>0</sub>), but it has not reached adsorption saturation yet. It shows that there are some mesoporous and macroporous in the material, and the volume of macroporous filling is caused by capillary condensation.

The adsorption lag exists in the range from 0.4 to 1.0 (p/p<sub>0</sub>), which is mainly due to the different mesoporous structure of porous materials. According to IUPAC classification criteria, this kind of hysteresis loop belongs to H3 type, indicating that the pore formed by diatomite is open at both ends with irregular pore structure characteristics, and the pore structure possess the characteristics of slit-like pore with parallel wall containing many other forms pores. This is in accordance with the pore structure of the opening of diatomite under SEM. Figure 3b shows the relationship between pore size and pore volume of diatomite. From Fig. 3b, it can be seen that the pore volume of DI-2 is larger than that of DI-1, which can be ascribed to the increase of pore volume of diatomite after calcination, acid leaching and alkali leaching.

### 4.3 XRD and morphology of diatomite, MWCNs and MWCNs-O, PCMs-M-D

Figure 4 is the XRD patterns of the PCMs, PCMs-M-D, DI-2. Except for the PCMs, THE MWCNs-O and DI-2 are existed in the PCMs-M-D, demonstrating that the DI-2 can adsorb the PCMs-M effectively.

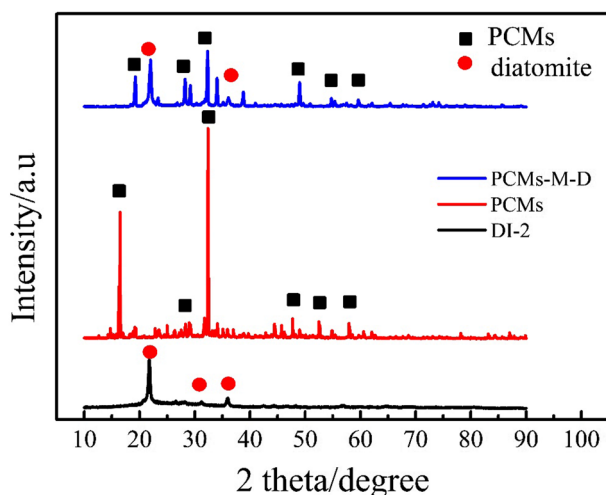


Fig. 4 XRD patterns of PCMs-M-D, PCMs, DI-2

Figure 5 is a SEM picture of DI-1 and DI-2. It can be seen from Fig. 5a that DI-1 is composed of porous disc structure. The pore structure of the disc structure is clear and visible. There are more debris on the surface and some pore structures are blocked. Figure 5b shows the porous structure of calcined and acid-alkali treated diatomite (DI-2). From Fig. 5b, it can be seen that the porous diatomite disc structure is well preserved and the pore size is obviously increased. It presents the state of through-hole at both ends. The pore structure changed from round to irregular round, because the main component of diatomite is SiO<sub>2</sub>. SiO<sub>2</sub> reacts with NaOH, some SiO<sub>2</sub> is dissolved, and the pore size is further increased.

The SEM images of MWCNTs and MWCNTs-O are displayed in Fig. 5 c and d. MWCNTs have a dark sink surface after being photographed by SEM, while that of the MWCNTs after oxidation treatment is glossy. Moreover, the length is not changed. Interestingly, it can be found that MWCNTs are intricately hovering together, and there are many prominent small pieces on the surface which are the aggregation sites of carboxyl groups.

Figure 5e–g is a SEM image of PCMs-M-D. The crystalline PCMs-M-D with burr flower-like morphology is adsorbed by the pore and filled almost all the pore of DI-2, demonstrating that DI-2 could adsorb PCMs-M well and makes the PCMs-M-D adhere to its matrix to crystallize.

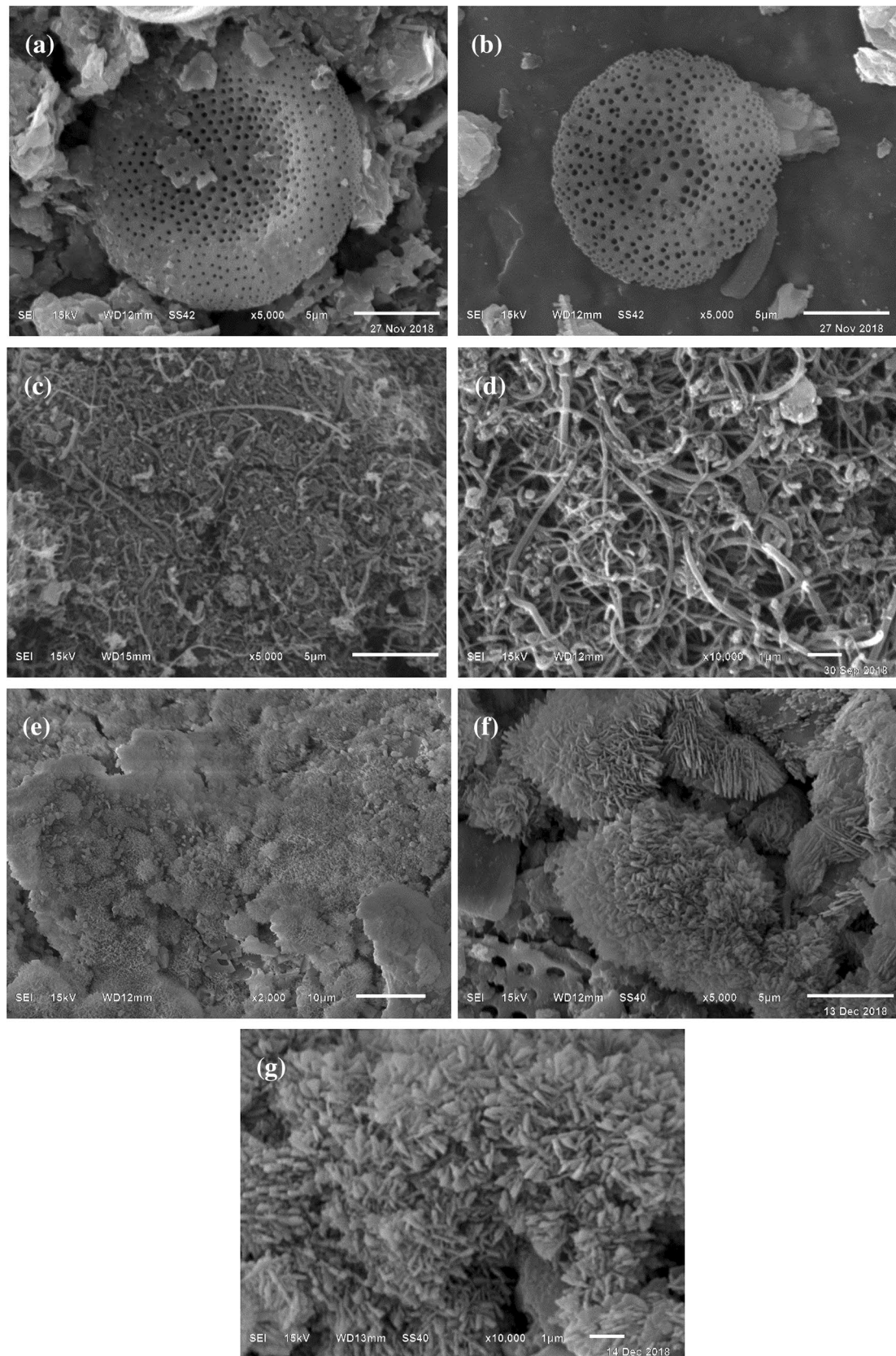
### 4.4 Analysis of thermal conductivity

Figure 6 displays the thermal conductivity diagram of PCMs and PCMs-M-D, showing that the highest thermal conductivity of PCMs-M-D is 0.97 W m<sup>-1</sup> K<sup>-1</sup> at 20 °C, which is much higher than that of the PCMs, resulting from the existence of the hydrophilic MWCNs with outstanding thermal conductivity in PCMs-M-D. In addition, during the preparation of PCMs-M-D by adsorption of DI-2 onto PCMs, the surface of PCMs and DI-2 combines via van der Waals to form a unified structure, enabling the PCMs-M-D transfer heat through lattice vibration and enhance the thermal conductivity.

### 4.5 Supercooling analysis

The T-history properties of PCMs and PCMs-M-D were investigated and the results are shown in Fig. 7. The supercooling degree of PCMs is 0.4 °C while the PCMs-M-D reveals negligible supercooling degree. The nucleation principle of PCMs-M-D can be explained by heterostructure nucleation theory. The PCMs tend to nucleate adhering to the DI-2 that exists in the mother liquor of PCMs, thus greatly reducing the the nucleation success and hence the degree of undercooling in the nucleation process. The results are in accordance with the SEM images





**Fig. 5** SEM images of **a** DI-1, **b** DI-2, **c** MWCNs, **d** MWCNs-O, and **e–g** PCMs-M-D

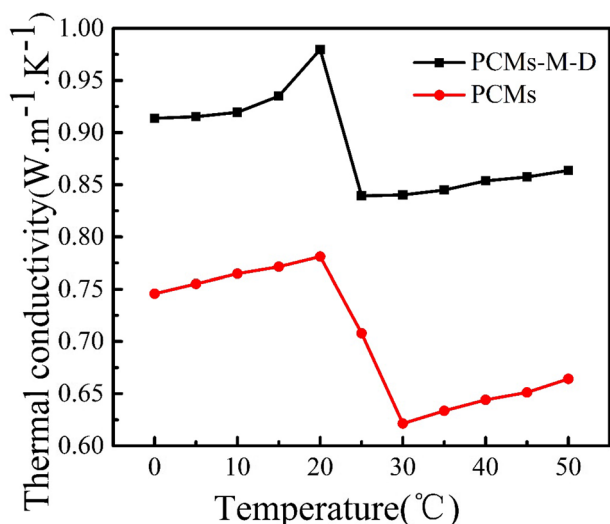


Fig. 6 Thermal conductivity of PCMs and PCMs-M-D

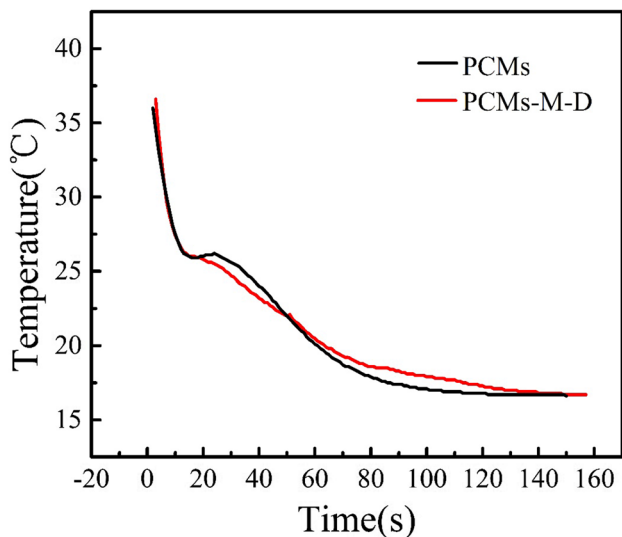


Fig. 7 T-history curves of PCMs and PCMs-M-D

which revealing that PCMs nucleated adhering to DI-2 and formed a layer of hairy spherical crystals on the surface.

#### 4.6 DSC characteristics

The phase transformation properties of phase change energy storage materials are described by melting and solidification initiation temperatures and latent heat of phase transformation. Figure 8 shows the thermal properties of PCMs and PCMs-M-D and the corresponding thermal characteristics are summarized in Table 1. It can be seen that, the  $T_{om}$  (Initial dissolution temperature),  $T_{em}$  (Termination dissolution temperature),  $\Delta H_m$  (Melting

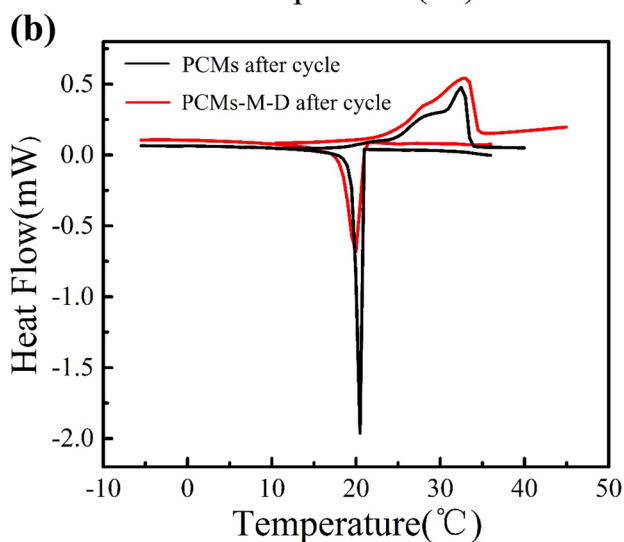
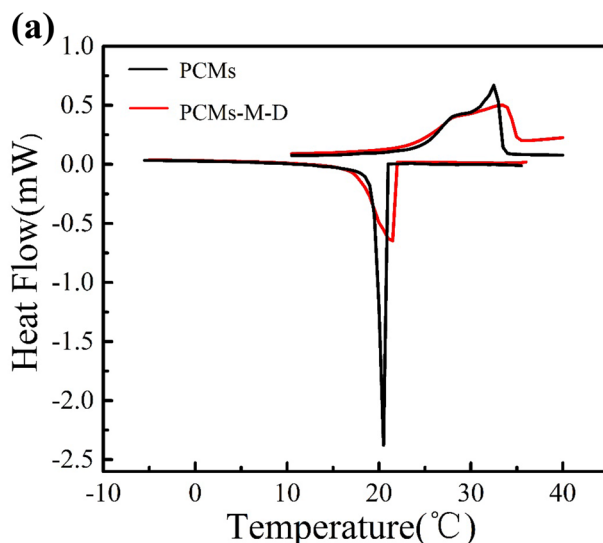


Fig. 8 DSC curves of PCMs and PCMs-M-D: **a** before, and **b** after 100 cycles

latent heat),  $T_{oc}$  (Initial solidification temperature),  $T_{ec}$  (Termination solidification temperature),  $\Delta H_c$  (Solidification latent heat) of PCMs are 24.6 °C, 33.4 °C, 175.2 J g<sup>-1</sup>, 20.7 °C, 19.6 °C, and 124.7 J g<sup>-1</sup>, respectively. The  $T_{om}$ ,  $T_{em}$ ,  $\Delta H_m$ ,  $T_{oc}$ ,  $T_{ec}$ ,  $\Delta H_c$  of PCMs-M-D are 24.5 °C, 34.3 °C, 146.6 J g<sup>-1</sup>, 21.7 °C, 17.3 °C, and 116.6 J g<sup>-1</sup>, respectively. After 100 heating (40 °C) and cooling (-5 °C) experiments, the  $T_{om}$ ,  $T_{em}$ ,  $\Delta H_m$ ,  $T_{oc}$ ,  $T_{ec}$ ,  $\Delta H_c$  of PCMs are 24.1 °C, 33.5 °C, 130.2 J g<sup>-1</sup>, 20.6 °C, 19.7 °C, 89.3 J g<sup>-1</sup>, respectively. The  $T_{om}$ ,  $T_{em}$ ,  $\Delta H_m$ ,  $T_{oc}$ ,  $T_{ec}$ ,  $\Delta H_c$  of PCMs-M-D after cycle are 24.6 °C, 35 °C, 144.5 J g<sup>-1</sup>, 20.9 °C, 18.2 °C, 103.6 J g<sup>-1</sup>, respectively. After 100 phase change cycles, the melting latent heat loss and the solidification latent heat loss of PCMs-M-D were 1.43% and 11.15%, respectively, which is obviously smaller than that of the PCMs with 26.68% melting latent heat loss and 28.39% solidification latent

**Table 1** Thermal characteristics of PCMs and PCMS-M-D

Samples	$T_{om}$ (°C)	$T_{em}$ (°C)	$\Delta H_m$ (J g <sup>-1</sup> )	$T_{oc}$ (°C)	$T_{ec}$ (°C)	$\Delta H_c$ (J g <sup>-1</sup> )	Heat loss rate
PCMs	24.6	33.4	175.2	20.7	19.6	124.7	/
PCMs-M-D	24.5	34.3	146.6	21.7	17.3	116.6	/
PCMs after cycle	24.1	33.5	130.2	20.6	19.7	89.3	26.68% 28.39%
PCMs-M-D after cycle	24.6	35	144.5	20.9	18.2	103.6	1.43% 11.15%

heat loss. With the adding of DI-2 and adsorbing PCMs via porous materials, PCMs can be well impregnated in the porous structure of diatomite under the action of capillary force and surface tension, which can reduce the stratification of phase change energy storage materials and adhere to the crystallization of porous structure, leading to the good cyclic stability of PCMs-M-D.

## 5 Conclusions

Based on the above discussion, the following conclusions can be drawn:

1. The DI-1 demonstrates large pore diameter with through-pore at both ends after being calcined, acid and alkali leached treatment. The Multi-walled carbon nanotubes contain carboxyl and hydroxyl groups through oxidizing process.
2. The awn nitrocellulose phase change shaped energy storage material was achieved through vacuum impregnating of DI-2 to adsorb MWCNTs, making it can be growth effectively attached to DI-2 during exothermic crystallization, and efficiently compatible with MWCNTs during endothermic dissolution.
3. PCMs-M-D has almost no supercooling degree, and the thermal conductivity increased to 0.97 W m<sup>-1</sup> K<sup>-1</sup> at 20 °C. After 100 cycles of phase change, the melting latent heat loss of mont-nitro composite is 1.43% and that of the solidification is 11.15%, respectively, demonstrating good thermal storage and chemical stability.

**Acknowledgements** The authors thank the research funds of Science and Technology Department Foundation of Qinghai Province (2015-Z-Y02,2016-Z-Y02), Qinghai Thousand Talents Program(724112), State Key Laboratory of Wuhan University of Technology(2017-KF-4).

## Compliance with ethical standards

**Conflict of interest** The authors declare that they have no conflict of interest.

## References

1. Shirvanimoghaddam K, Hamim SU, Karbalaee Akbari M, Fakhrhosseini SM, Khayyam H, Pakseresht AH et al (2017) Carbon fiber reinforced metal matrix composites: fabrication processes and properties. *Compos A Appl Sci Manuf* 92:70–96. <https://doi.org/10.1016/j.compositesa.2016.10.032>
2. Milián YE, Gutiérrez A, Grágeda M, Ushak S (2017) A review on encapsulation techniques for inorganic phase change materials and the influence on their thermophysical properties. *Renew Sustain Energy Rev* 73:983–999. <https://doi.org/10.1016/j.rser.2017.01.159>
3. Wang X, Guo Y, Su J, Zhang X, Han N, Wang X (2018) Microstructure and thermal reliability of microcapsules containing phase change material with self-assembled graphene/organic nano-hybrid shells. *Nanomaterials* (Basel). <https://doi.org/10.3390/nano8060364>
4. Ibrahim NI, Al-Sulaiman FA, Rahman S, Yilbas BS, Sahin AZ (2017) Heat transfer enhancement of phase change materials for thermal energy storage applications: a critical review. *Renew Sustain Energy Rev* 74:26–50. <https://doi.org/10.1016/j.rser.2017.01.169>
5. Waqas A, Ud DZ (2013) Phase change material (PCM) storage for free cooling of buildings—a review. *Renew Sustain Energy Rev* 18:607–625. <https://doi.org/10.1016/j.rser.2012.10.034>
6. Jiang DH, Li AG, Shi FE, Ren RS (2010) Mineral sepiolite energy-saving residential materials. *Adv Mater Res* 178:185–190. <https://doi.org/10.4028/www.scientific.net/AMR.178.185>
7. Konuklu Y, Ersoy O (2016) Preparation and characterization of sepiolite-based phase change material nanocomposites for thermal energy storage. *Appl Therm Eng* 107:575–582. <https://doi.org/10.1016/j.applthermaleng.2016.07.012>
8. Ali Memon S, Yiu Lo T, Shi X, Barbhuiya S, Cui H (2013) Preparation, characterization and thermal properties of Lauryl alcohol/Kaolin as novel form-stable composite phase change material for thermal energy storage in buildings. *Appl Therm Eng* 59(1–2):336–347. <https://doi.org/10.1016/j.appltherma.2013.05.015>
9. Li W, Huang R, Zong J, Zhang X (2017) Microencapsulation and morphological characterization of renewable microencapsulated phase-change materials with cellulose diacetate shell. *ChemistrySelect* 2(21):5917–5923. <https://doi.org/10.1002/slct.201701078>
10. Guo X, Huang Y, Cao J (2018) Performance of a thermal energy storage composite by incorporating diatomite stabilized paraffin as phase change material. *Energy Build* 158:1257–1265. <https://doi.org/10.1016/j.enbuild.2017.11.032>
11. Zhang X, Li X, Zhou Y, Hai C, Shen Y, Ren X et al (2017) Calcium chloride hexahydrate/diatomite/paraffin as composite shape-stabilized phase-change material for thermal energy storage. *Energy Fuels* 32(1):916–921. <https://doi.org/10.1021/acs.energyfuels.7b02866>
12. Jiang ZP, Tie SN (2015) Preparation and properties of Glauber's salt-based composite phase change materials by

- physical method. *J Synth Cryst* 12(44):3639–3645. <https://doi.org/10.16553/j.cnki.issn1000-985x.2015.12.050>
13. Liu X, Tie S, Tie J (2016) Energy storage properties of mans nitro phase transition materials of multi-walled carbon nano-tubes of greenhouse. *Trans Chin Soc Agric Eng* 32(6):226–231. <https://doi.org/10.11975/j.issn.1002-6819.2016.06.031>

**Publisher's Note** Springer Nature remains neutral with regard to jurisdictional claims in published maps and institutional affiliations.